Article

An Early Study on the Synthesis of Lignin-Graft-(Net-Poly(acrylamide-co-N,N′methylenebisacrylamide)), Characterization of the Produced Copolymer, and Evaluation of Its Performance as Adsorbent for Lead Removal from Wastewater Purposes

María Fernanda Munguía-Quintero [ID], Miguel Ángel Vega-Hernández, Alberto Rosas-Aburto [ID], Martín Guillermo Hernández-Luna, Simón López-Ramírez [ID], José Fernando Barragán-Aroche [ID] and Eduardo Vivaldo-Lima *[ID]

Facultad de Química, Departamento de Ingeniería Química, Universidad Nacional Autónoma de México, Ciudad de México 04510, Mexico; fernandamunguiaq@comunidad.unam.mx (M.F.M.-Q.); miguel.angel.vega@comunidad.unam.mx (M.Á.V.-H.); alberto_rosas_aburto@comunidad.unam.mx (A.R.-A.); martinhl@unam.mx (M.G.H.-L.); slr@unam.mx (S.L.-R.); jfba@unam.mx (J.F.B.-A.)
* Correspondence: vivaldo@unam.mx

Abstract: A lignin-graft-(net-poly(acrylamide-co-N,N′methylenebisacrylamide)) copolymer was synthesized by conventional free-radical crosslinking copolymerization using conventional and microwave heating. Grafting of the polymer network onto lignin was confirmed by Fourier transform infrared spectroscopy (FTIR), nuclear magnetic resonance spectroscopy (NMR), scanning electron microscopy (SEM)/energy dispersive spectroscopy (EDS), thermogravimetric analysis (TGA), and elemental analysis. The performance of the modified materials for the removal of lead from water was evaluated. The materials obtained by the two types of heating showed excellent removal efficiencies: sample HLigAM4h, 96%; and sample HLigAMMW5, 86%. The maximum adsorption capacity of HLigAM4h was 209.82 mg g^{-1}. The obtained copolymer (sample HLigAM4h) was characterized by X-ray photoelectron spectroscopy (XPS) and SEM/EDS after its evaluation as an adsorbent, which confirm the adsorption of Pb^{2+}. This is the first of a series of studies on the topic, of a preliminary nature, with several other ones coming up in due time.

Keywords: polymer modification; polymer grafting; adsorbents; lead adsorption

1. Introduction

The use of natural biopolymers, such as lignocellulosic biomasses or its components, in different important technological areas is a viable option to decrease waste generation problems and reduce or replace the use of synthetic polymers. One of the main components of lignocellulosic biomasses is lignin, which is the second most abundant source of renewable materials in nature, after cellulose. Lignin has a heterogeneous structure composed mainly of three phenylpropane units: guaiacyl (G unit), syringyl (S unit), and p-hydroxyphenyl (H unit), where the difference is the degree of methoxyl substitution on the phenolic ring [1,2]. Although vast amounts of lignocellulosic biomasses are used in low added-values applications, such as composting, animal feeding, or burnt for energy producing purposes, their use for more appealing applications has grown in importance in the last few years [3]. If more sophisticated biopolymers are required, some of these applications require to chemically modify the starting biopolymers obtained from the lignocellulosic biomasses. Numerous physical and chemical methods can be used to perform chemical modifications to add industrial value to lignin, or develop new polymeric materials, due to the large number of functional groups present in lignin and its physical properties [4,5].

Functionalization and chemical modification of biopolymers, including lignin, are very useful to improve the thermomechanical properties of these materials, which expand their uses [6]. Lignin and its derivatives can be easily modified from the primary phenol and hydroxyl groups, as well as the active hydrogen atom near the phenol group [7]. The chemical modification reactions of lignin define its structure, molecular weight, and number of functional groups. They also play a very important role on performance for different applications [8]. Chemical modification reactions that favorably modify lignin include methylation [9], amination [4], sulfonation [10], carboxylation [11], esterification [12], crosslinking [13], and graft copolymerization [14]. In graft copolymerization, lignin is covalently modified by polymer branches which improve the mechanical proprieties and thermal resistance of the (modified copolymer) material [14]. There are two main routes for the insertion of polymer chains onto lignin: (1) generation of new reactive sites within the lignin framework; and (2) modification or functionalization of the hydroxyl groups of lignin [15]. Reported applications of materials produced from grafting of vinyl polymers onto lignin include their use as additives for drilling fluids [16], flocculants [17], dye adsorbents [18], and adsorption of heavy metals [19], among others.

The flocculation efficiency of natural polymers in wastewater treatment processes is only moderate. Graft polymerization of vinyl monomers onto biopolymers has proven to be a remarkable method to enhance the flocculation performance of biopolymers [17,20]. Polyacrylamide (PAM) has been used as flocculant for the removal of different wastewater pollutants. This is possible due to its long chain structure, which contains charged amide groups that make it water soluble and impart hydrophilic properties. However, PAM is not derived from renewable sources [21,22]. Although slowly, PAM may decompose up to acrylamide monomer in a natural environment [23]. Furthermore, acrylamide residues result in biological neurotoxicity and potential risks of carcinogenesis [22]. Functionalization or copolymerization of PAM with another polymer or biopolymer can be used to reduce this problem.

Chen et al. [24] fabricated a chelating flocculant which consisted of a copolymer of polyacrylamide grafted onto maleoyl chitosan-mercapto acetic acid (PAM-g-M(CS-MA)). This flocculant had a removal efficiency of 93.90 and 92.47% for Cu and Cd, respectively. Feng et al. [22] prepared a graft copolymer of acrylamide onto carboxymethyl cellulose and used it for the removal of dyes from wastewater.

The adsorption of heavy metal ions, such as Cu^{2+}, Pb^{2+}, and Cr^{3+}, generally depends on the interaction between the metal ions and the reactive groups present in the adsorbent. These reactive groups include hydroxyl (-OH), amino ($-NH_2$), carboxylic (-COOH), and thiol (-SH). If the adsorbent structure contains a large amount of these groups, high adsorption efficiencies can be achieved [25].

The adsorption capacity of unmodified lignin is usually limited by the low amount of amino, sulfo, or hydroxyl groups. The introduction of these functional groups into lignin-based adsorbents by grafting of polymers whose monomer units contain such functional groups into lignin, is expected to improve the adsorption capacity of heavy metal ions [26].

The grafting of synthetic polymers onto lignin or lignin derivatives by free radical polymerization to produce adsorbents has been evaluated. Some of the reported grafted polymers include polyethyleneimine [27,28] and poly(acrylic acid), which result in good adsorption efficiencies for different heavy metals ions, such as Ni(II), Cd(II), As(V), Hg(II), Cu(II), Cr(VI), Co, and Pb(II). Ge et al. [29] prepared lignin microspheres with abundant amine functional groups by grafting polyethylenimine (PEI) onto the biopolymer, reaching an adsorption capacity of 33.9 mg g^{-1} for Pb^{2+}. Liu et al. [19] prepared a composite hydrogel by grafting poly(acrylic acid) onto acid-pretreated alkali lignin; the material had an adsorption capacity of 1.076 mmol g^{-1} for Pb^{2+}. Jiao et al. [30] fabricated a sulfomethylated lignin-grafted-poly(acrylic acid) adsorbent by ultrasonic-assisted free-radical polymerization. The material had an adsorption capacity of 344.85 mg of Pb^{2+} per gram of adsorbent.

In this contribution, we report the synthesis of a grafted copolymer based on lignin and PAM, using conventional and microwave heating. PAM was grafted onto lignin by crosslinking free radical copolymerization using N,N′methylenebisacrylamide as crosslinker. A crosslinked structure was chosen to prevent dissolution in water of the obtained material. The grafted copolymer was characterized by FTIR, NMR, TGA, SEM/EDS, XPS, and elemental analysis.

The grafted copolymer was evaluated in batch adsorption experiments for removal of Pb^{2+} from aqueous solutions. The adsorption efficiencies of Pb^{2+} in unmodified lignin, PAM, and in our crosslinked grafted material were compared, obtaining a significantly better performance when our material is used.

2. Materials and Methods

2.1. Materials

All chemicals used were of analytical reagent grade: Kraft lignin (CAS: 8068-05-1), N,N′-methylenebisacrylamide (99%), acrylamide (98%), and ammonium persulfate (APS, 98%), Lead (II) nitrate, all from Sigma-Aldrich (Toluca, México); sodium hydroxide (NaOH) and sulfuric acid (H_2SO_4), both from J.T. Baker® (Xalostoc, México).

2.2. Graft Copolymerization

2.2.1. Conventional Heating

The modified lignin was produced by combined grafting and crosslinking, following a free radical copolymerization chemical route [19]. First, lignin (1.0 g) was dissolved in 85 mL of NaOH (1.25 M). Ammonium persulfate (0.1 g) and N, N′-methylenebisacrylamide (0.2 g) were added as initiator and crosslinker, respectively. The solution was heated at 60 °C and stirred for 30 min. Then, acrylamide (2.0 g) was added and allowed to react for 2, 4, and 24 h. The reaction was terminated by reducing the temperature to 20 °C. After finishing the reaction, 200 mL of water was added and acidified with H_2SO_4 until pH 1.5 was obtained. The precipitated material was separated by centrifugation (5000 rpm), washed with water, and dried at 60 °C, for 24 h [17,19,31]. The synthetized materials, which correspond to a 2, 4, and 24 h reaction time, were named HLigAM2h, HLigAM4h, and HLigAM24h, respectively. The homopolymer (PAM) was synthesized under the same conditions, without lignin.

Grafting yield (*Y*, mass %) and grafting ratio (*GR*, mol %) were calculated using Equations (1) and (2), respectively [17,32,33].

$$Y(mass\ \%) = \frac{W_2}{W_0 - W_1}\ 100 \tag{1}$$

$$GR\ (mol\ \%) = \frac{V_1 MW_{AM}}{100 MW_N - V_1 MW_{AM}}\ 100 \tag{2}$$

where W_0 and W_1 are masses (g) of lignin and *AM*, respectively, and W_2 is mass of copolymer (g). V_1 in Equation (2) is nitrogen gain obtained from elemental analysis measurements by subtracting nitrogen content present in unmodified lignin (*N*, %). MW_{AM} and MW_N are acrylamide and nitrogen molecular weights (g mol^{-1}), respectively.

2.2.2. Microwave Heating

The same amounts of lignin, ammonium persulfate, N,N-methylene bisacrylamide and a solution of NaOH (0.5 M) as a solvent were added into a flask. After stirring for 5 min, acrylamide was added; stirring continued for 5 more min. Lignin modification was carried out in a glass container placed in a microwave oven (StartSYNTH, Milestone, Shelton, Connecticut, USA) at a power of 100 W, for 5 min. Reactions at other times were also carried out, but 5 min provided the best results. Once the reaction time was reached, the reaction was stopped, and the same separation procedure was followed. The synthetized material was named HLigAMMW5.

2.2.3. Characterization

Kraft Lignin, PAM and the modified materials were characterized by Fourier transform infrared spectroscopy (FTIR), nuclear magnetic resonance spectroscopy (NMR), scanning electron microscopy (SEM), thermogravimetric analysis (TGA), X-ray photoelectron spectroscopy (XPS), and elemental analysis, to confirm that grafting took place, and to evaluate changes in the structure of lignin. FTIR spectra were recorded in a range of wave numbers from 4000 to 650 cm^{-1}, using an M series, Midac Corporation spectrometer (Westfield, MA, USA). Potassium bromide (KBr) pellets containing the samples were prepared by mixing and pressing 2 mg of dried sample with 200 mg of KBr. ^{1}H NMR spectra were recorded using 400 MHz, Varian, MR, USA, and 600 MHz, JEOL, ECZ600R spectrometers, and ^{13}C NMR spectra were recorded also using a 400 MHz, Varian, MR, Santa Clara, CA, USA, spectrometer, operating at 151 MHz. The samples were dissolved in deuterated dimethyl sulfoxide (DMSO-d6) and analyzed. SEM images and energy dispersive spectroscopy (EDS) were obtained using a JSM-5900-LV, JEOL microscope, Peabody, MA, USA. TGA analyses were performed under nitrogen atmosphere by increasing temperature from 30 to 900 °C at a heating rate of 5 °C min^{-1}, using a TGA550, Discovery Series, equipment, USA. XPS was used to calculate elemental compositions and analyze chemical states; a VERSAPROBE II, Physical Electronics, Chanhassen, MI, USA, spectrometer was used. A Flash 200, FPD 800, Thermo Scientific elemental analyzer, Waltham, MA, USA, was also used for elemental analysis of samples.

2.2.4. Adsorption of Pb^{2+}

Adsorption of Pb^{2+} batch experiments were performed at 25 °C, pH of 5.5, stirring of 240 rpm, as well as variable Pb^{2+} initial concentration and contact time. Several reports confirm that the optimal pH for Pb^{2+} removal lies between 5 and 6 [26,34–36]. Adsorption capacity at low pHs is limited due to the protonation of -NH, -OH and -COOH, which are potential adsorption sites in lignin [31,36]. On the other hand, a high pH results in the precipitation of Pb(OH)$_2$ and Pb(OH)$_4$ $^{2-}$, which may adversely affect the adsorption process and reduce the adsorption capacity [26,36,37]. Samples of the modified lignin copolymer (0.1 g) were soaked in a lead nitrate solution (100 mL) using a flask, for 2 h. Samples of 5 mL supernatant solution were separated and then filtered through 110 mm filter paper Whatman$^\circledR$ every 20 min. The concentrations of Pb^{2+} after adsorption were measured by using an atomic absorption spectrophotometer (PinAAcle 900 Serie AA, Perkin Elmer Spectrometers). The adsorption capacity (*q*, mg g^{-1}) and the removal efficiency (*R*, %) of Pb^{2+} ions were calculated according to the following expressions:

$$q\left(\frac{mg}{g}\right) = \frac{(C_0 - C_e)\ V}{m} \tag{3}$$

$$R(\%) = \frac{(C_0 - C_e)}{C_0} \times 100 \tag{4}$$

where C_0 and C_e (mg L^{-1}) represent the initial and equilibrium concentrations of Pb^{2+} ions, respectively; *V* (L) is the volume of the solution and *m* (g) is the amount of lignin-modified copolymer (adsorbent).

3. Results and Discussion

3.1. Lignin Modifications

Lignin-graft-(net-poly(acrylamide-co-N,N′methylenebisacrylamide)) copolymers with different compositions were synthesized by crosslinking free radical copolymerization. As explained earlier, a polymer network structure of the grafted copolymer was sought to prevent dissolution in water of the modified material. The proposed reaction route is shown in Figure 1. Thermal (conventional) heating has been used in several reports where the reaction time is typically 24 h [14,16,38]. The use of microwave heating has been reported in the synthesis of some copolymers, decreasing the reaction time, and obtaining

higher conversions [39,40]. In this contribution, both routes were used. Thermal heating was carried out at three different reaction times (2, 4, and 24 h). Microwave heating was conducted at 1, 3, 5, and 7 min; but the best results were obtained at 5 min of reaction. The yields obtained in samples HLigAM4h and HLigAMMW5 were 26.19 and 25.63%, respectively. Likewise, the corresponding grafting ratios obtained for those samples were 4.56 and 4.01%, respectively.
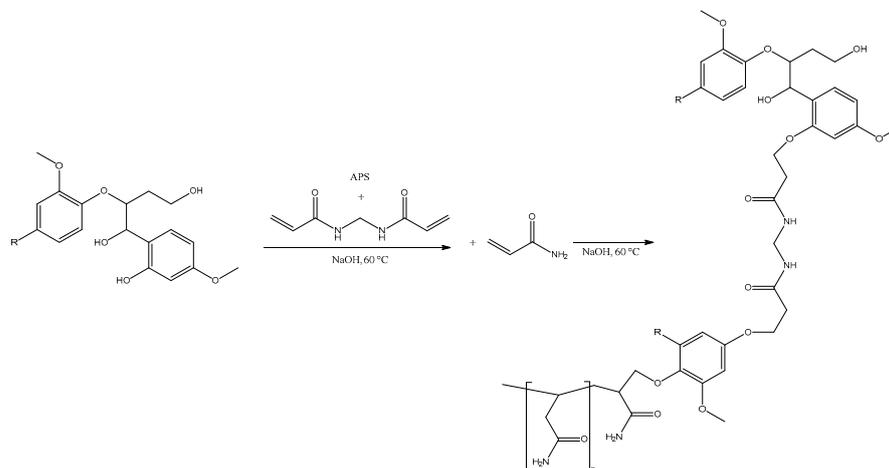
Figure 1. Chemical route for the grafting of crosslinked PAM onto lignin.

3.2. Characterization of Starting and Modifed Lignin Copolymers

The FTIR spectra for PAM (A), Lignin (B), HligAM4h (C), HLigAM24h (D), and HLigAMMW5 (E) are shown in Figure 2. The bands around 1600, 1515, and 1420 cm^{-1} for lignin were assigned to the skeletal vibration of aromatic rings [41,42] and the absorption bands at 1261, 1241, and 1125 cm^{-1} were attributed to the guaiacyl, gyringyl, and ether bonds of lignin [30]. These absorption bands are clearly seen in the spectra for HLigAM4h, HLigAM24h, and HLigAMMW5, which indicates that the aromatic structure of lignin was not destroyed or changed during de copolymerization [36]. In the case of PAM, the bands at 2960, 1720, and 1660 cm^{-1} were attributed to N–H, C=O and C=C stretching vibrations, respectively [43]. Notably, in the spectra corresponding to HLigAM4h, HligAM4h and HLigAMMW5 a new adsorption peak around 1720 cm^{-1} was observed, which was attributed to the carbonyl bond from an amide bond, was observed. This confirms that PAM was successfully grafted onto lignin [8,16,43].
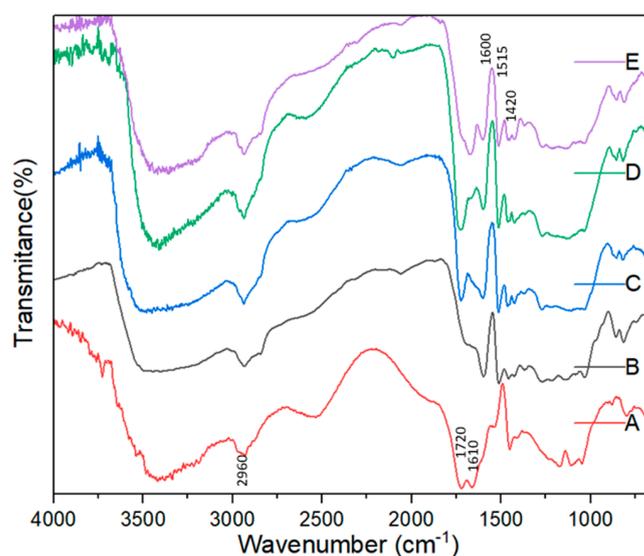
**Figure 2.** FTIR spectra for lignin, PAM, and the synthesized copolymers.

Figure 3 shows TGA (Figure 3A) and DTGA (Figure 3B) results for lignin, PAM, HLigAM4h, and HLigAMMW5. Weight losses in the range 40 to 150 °C correspond to water, solvent, and other small molecules. As observed, lignin decomposes over a wide temperature range, from 150 to 500 °C, due to its heterogeneity and the absence of a defined structure [17]. In this temperature range, the carbon–carbon bonds between lignin units and the side chain of aromatic rings are broken [44,45]. At 500 °C, lignin has lost 56.72% of its mass, while copolymers HLigAM4h and HLigAMMW5 have lost 35.69 and 35.76% of their masses, respectively. This result indicates that the modified lignin copolymers have better thermal stabilities than lignin and PAM. The maximum mass loss temperature is 554 °C for lignin, 824 °C for HLigAM4h and 831 °C for HLigAMMW5. It is also observed in Figure 3 that lignin losses mass much more pronouncedly than modified lignin copolymers. This result suggests that unmodified lignin may be severely affected by the harsh conditions of the grafting process.
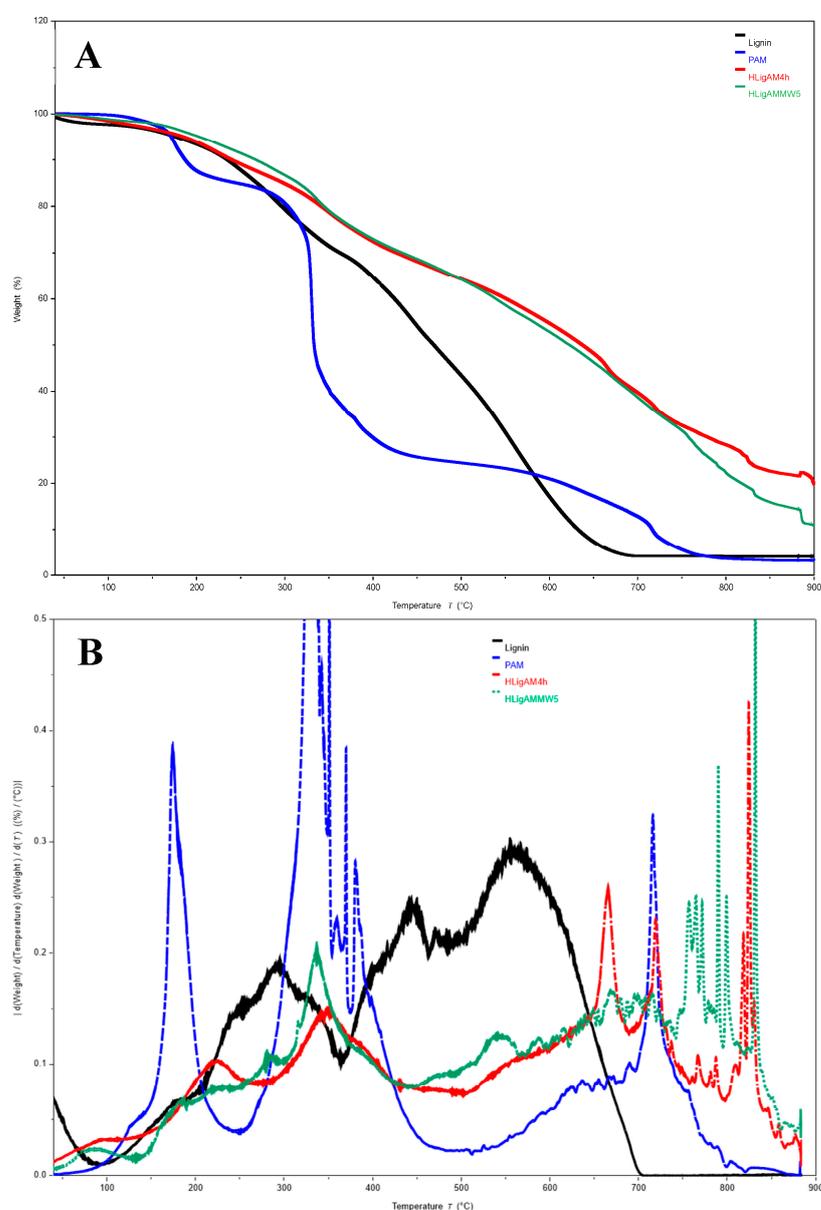

Figure 3. TGA (**A**) and DTGA (**B**) thermogravimetric curves for Lignin, PAM, and modified lignin.

Figure 4 shows 400 MHz ^{1}H-NMR spectra for lignin and HLigAM4h; Figure 5 shows 600 MHz ^{1}H-NMR spectra for lignin and HligAM24h; and Figure 6 shows 600 MHz

^{1}H-NMR spectra for lignin and HLigAMMW5. Chemical shifts of the aromatic rings (p-coumaryl, coniferyl, and sinapyl), vinylic protons [2], and methoxy group (OCH$_3$) [46] were identified in the lignin spectra. In the spectra for the modified copolymers, chemical shifts from 7.03 to 7.21 ppm are attributed to the presence of PAM. Shifts between 4.0 and 4.6 are attributed to different PAM branches grafted onto lignin. The shifts related to the CH$_2$ group of PAM linked to the phenolic O atom of lignin [8,18], or to the CH$_2$ group linked to O in the crosslinker, are also observed. Shifts at 4.6 ppm can be attributed to protons associated with grafted PAM, but bonded to other phenolic structures, different from that proposed in Figure 1. The new signals between 2.7 and 2.2 ppm can be attributed to the CH and CH$_2$ groups of PAM. Sample HLigAMMW5 exhibits new shifts between 6.2 to 6.0 ppm, compared to bare lignin. These shifts are associated with hydroxyl groups, mainly in sugar units (HO-) [47]. Since Kraft lignin has no shifts in this region, they should have appeared after the grafting process, possibly by formation of a carboxylate group from hydrolysis of the amide group. These shifts might be attributable to the crosslinking process through the phenolic group of the crosslinking agent with the immediate breaking of the bond, where pendant HO- groups remain. Aromatic rings change with this bonding and breaking process, acquiring a quinoid conformation. Protons associated with these structures may show shifts from 6.2 to 5.7 ppm, according to the neighbor functional groups.
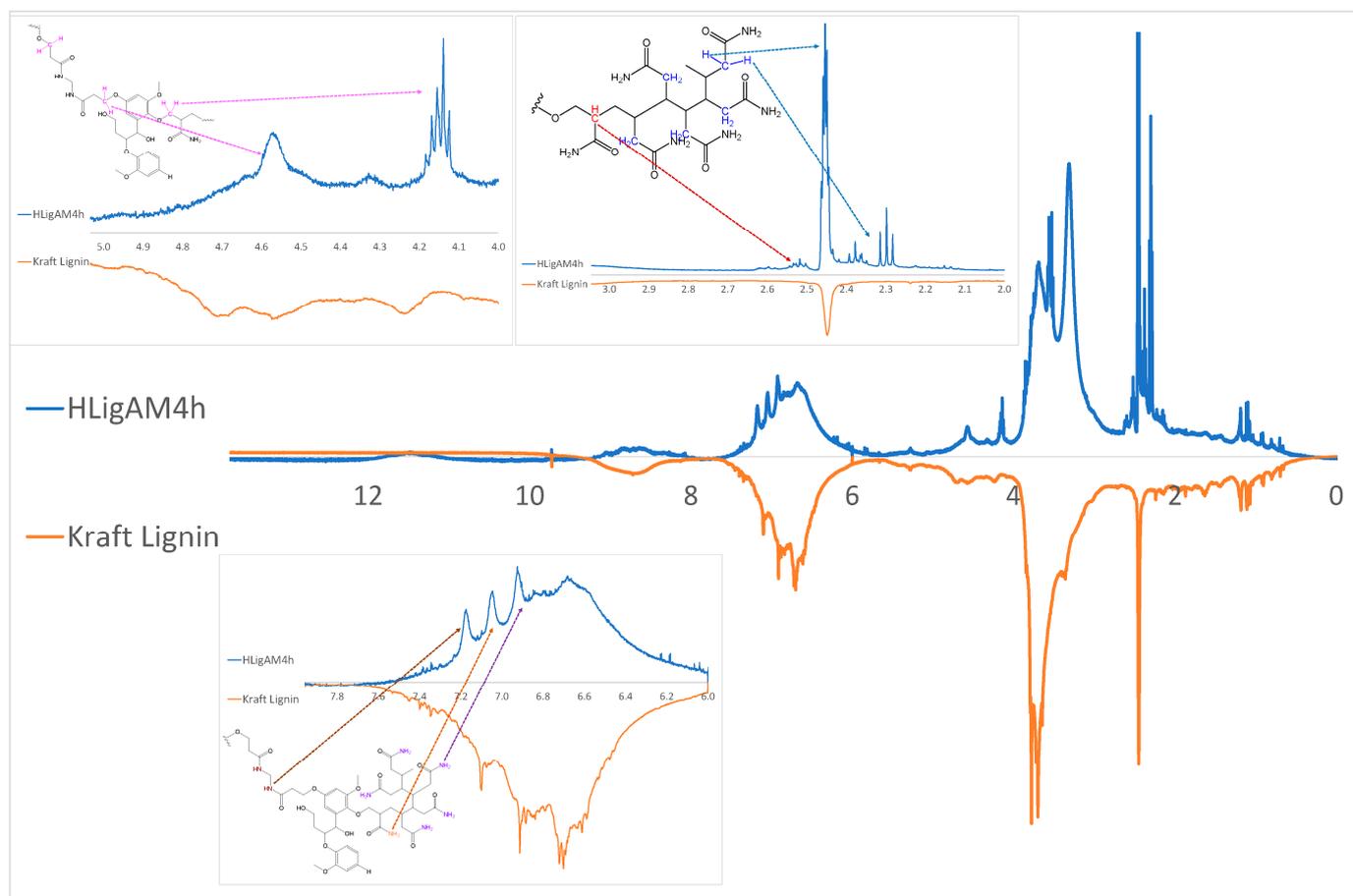
Figure 4. 400 MHz ^{1}H NMR spectra for lignin and sample HLigAM4h.
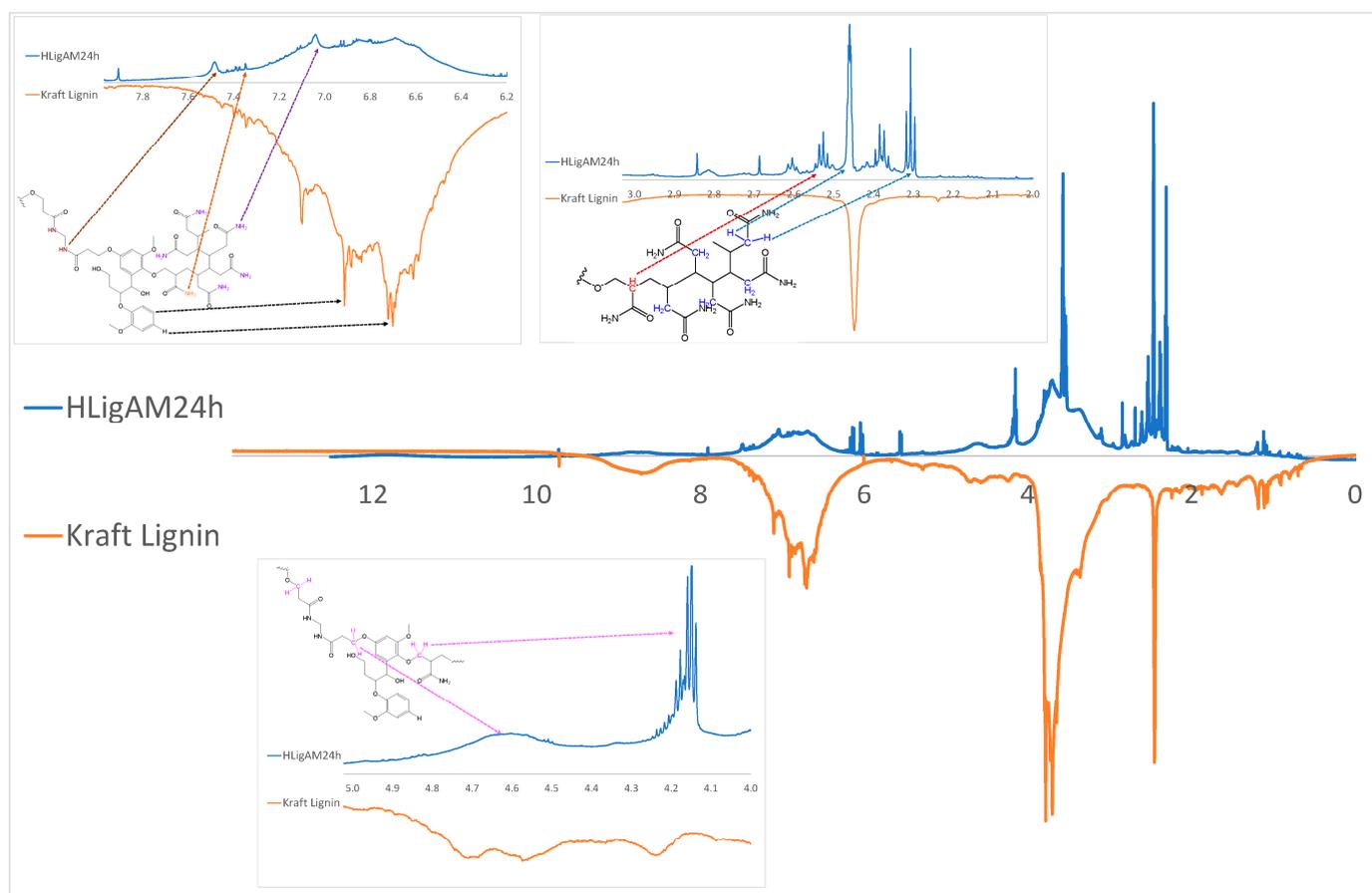
Figure 5. 400 MHz ^{1}H NMR spectra for lignin and 600 MHz ^{1}H NMR sample HLigAM24h.

The ^{13}C-NMR spectra for Lignin, HLigAM24h, and HLigAMMW5 are shown in Figure 7. The signal at 40 ppm corresponds to DMSO-d6. Methoxy groups are observed at 55 ppm. The carbon in the aromatic skeleton of lignin is observed from 110 to 170 ppm. The signals at 112 and 115 ppm are related to C2 and C5 of the guaiacyl unit; the signal at 130 ppm corresponds to C1, in the guaiacyl ring [2]. The new signals at 35, 38, 49, 57, and 66 ppm in the spectrum for HLigAM24h can be attributed to carbons from the CH and CH$_2$ groups of PAM [26]. The increase in the signals at 166, 171, and 172 ppm may be attributed to the carboxyl group [36].

SEM images and EDS analyses for lignin, HLigAM4h, and HLigAM4h with adsorbed lead (HLigAM4h-Pb) are shown in Figure 8. As observed, the surface of lignin was irregular and relatively fragmented. After grafting/crosslinking modification, the surface was more regular, with larger particles. An increase in oxygen and sodium is observed in the EDS spectrum. It is reported in different publications that the hydroxyl groups of lignin react with NaOH under alkaline conditions, generating a strong nucleophile, which serves as a catalyst for carboxylation reactions [36,48,49]. The increase in the percentage of Na in the modified materials suggests that this bond is present.

The results of elemental analysis for lignin, HLigAM4h, and HLigAMMW5 are shown in Table 1. As observed, the content of nitrogen and oxygen increased, which may be attributed to the amide groups (-CONH$_2$) of PAM, which was grafted onto the lignin backbone.
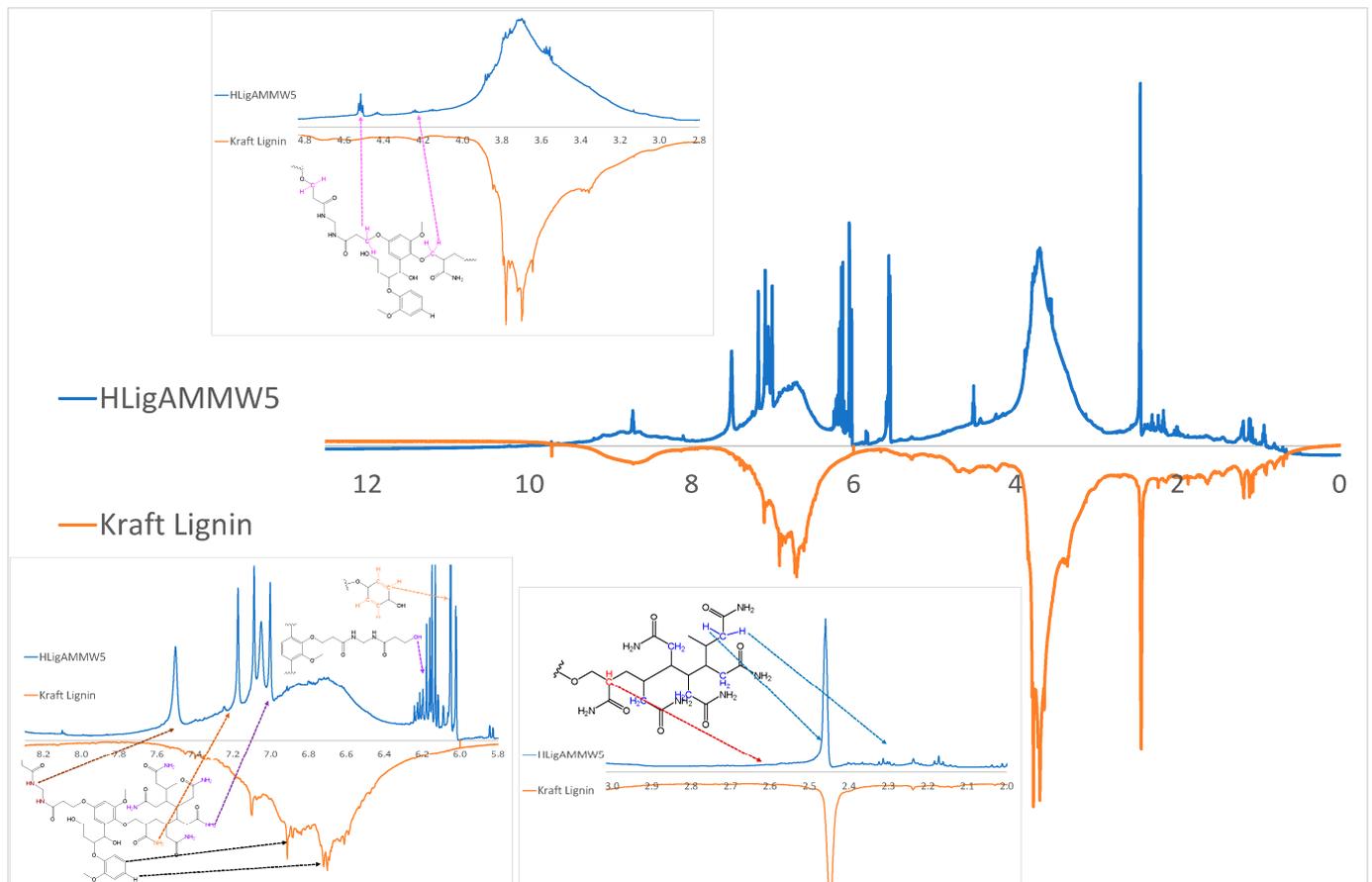
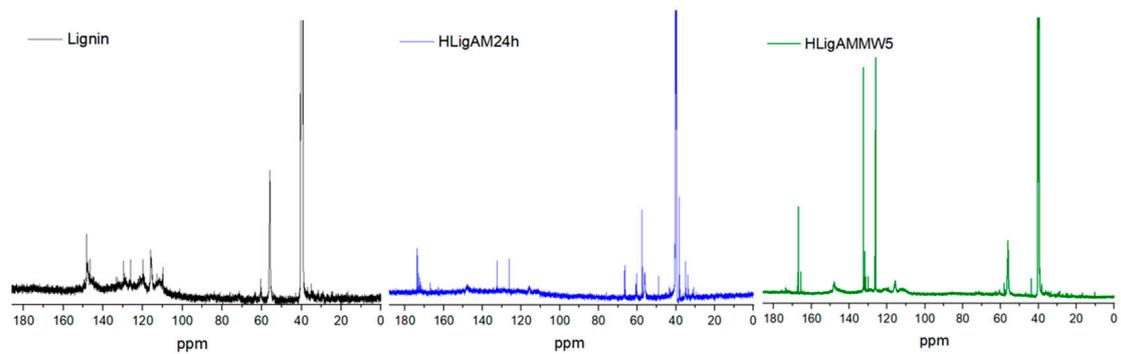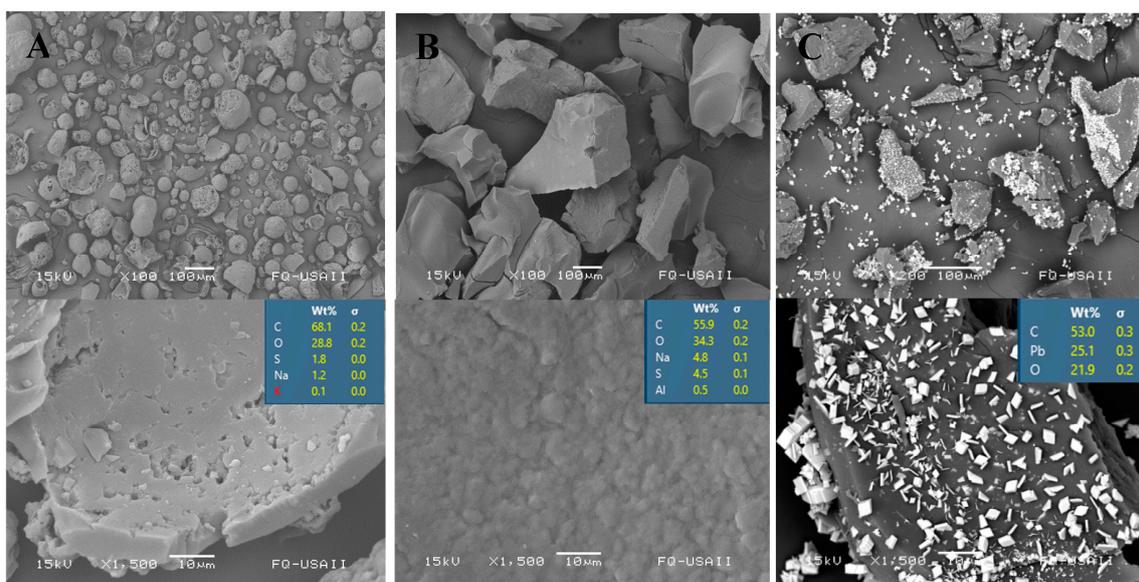**Figure 6.** 400 MHz ^{1}H NMR spectra for lignin and 600 MHz ^{1}H NMR sample HLigAMMW5.

Figure 7. ^{13}C NMR spectra of lignin and synthesized copolymers.

Figure 8. SEM images of lignin and HLigAM4h: (**A**) Kraft Lignin; (**B**) HLigAM4h; (**C**) HLigAM4h-Pb (evaluated in lead removal).

Table 1. Results of elemental analysis for lignin, HLigAM4h, and HLigAMMW5.

Material	H (%)	O (%)	H (%)	N (%)
Lignin	62.06 ± 0.105	27.10 ± 0.138	5.45 ± 0.018	1.71 ± 0.067
HLigAM4h	43.90 ± 0.169	35.19 ± 0.025	4.33 ± 0.075	2.57 ± 0.134
HLigAMMW5	53.12 ± 4.108	30.43 ± 0.172	4.99 ± 0.237	2.47 ± 0.061

3.3. Pb^{2+} Adsorption Experiments

3.3.1. Effect of Material and Likely Removal Mechanism

Pb^{2+} adsorption experiments were performed to evaluate the effect of lignin modification on Pb^{2+} removal efficiency from a water solution (80 mg/L of Pb^{2+}). Results are shown in Figure 9. Unmodified lignin had a removal efficiency of 43% while the removal efficiency of PAM was 73%, but unlike lignin, PAM dissolves in water. Copolymer HLigAM4h reached a 92% removal efficiency, almost 50% higher than unmodified lignin, with the additional advantage that it does not dissolve in water and its separation is easier. Adsorption capacities at 120 min of contact are 28.02, 55.40, and 74.33 mg g^{-1} for unmodified lignin, PAM, and HLigAM4h, respectively. Figure 8c shows images corresponding to HLigA4h-Pb. It is observed that lead particles adhered to the copolymer surface. Sodium content in HLigAM4h-Pb decreased almost entirely, which suggests that sodium may favor the removal of Pb^{2+}, as an ion exchange device [50,51]. Figure 10a shows XPS spectra before and after adsorption of Pb^{2+}. Characteristic peaks corresponding to carbon and oxygen are observed. Pb4f and Pb4d peaks can be observed after adsorption of Pb^{2+}, which indicates that Pb^{2+} has been adsorbed on the surfaces of the adsorbent in different binding forms [52]. XPS spectra for O 1s is shown in Figure 10c,d. The three peaks at 531.78, 530.61, and 529.59 eV that result from the deconvolution of O1s, for sample HLigAM4h, can be assigned to O-H, C=O, and C-O, respectively. The O-H and C=O peaks had a chemical shift at 533.01 and 531.37 eV after the adsorption experiment, which suggests that they are involved in the adsorption of Pb^{2+} [53]. A new peak at 527.27 eV was observed and assigned to the oxygen atom in Pb-O. The Pb4f XPS spectrum of Figure 10b can be divided into Pb4f5/2 (143.55 eV) and Pb47/2 (138.67 eV); these two peaks may be related to Pb-O and Pb-O-C, respectively [52,54].

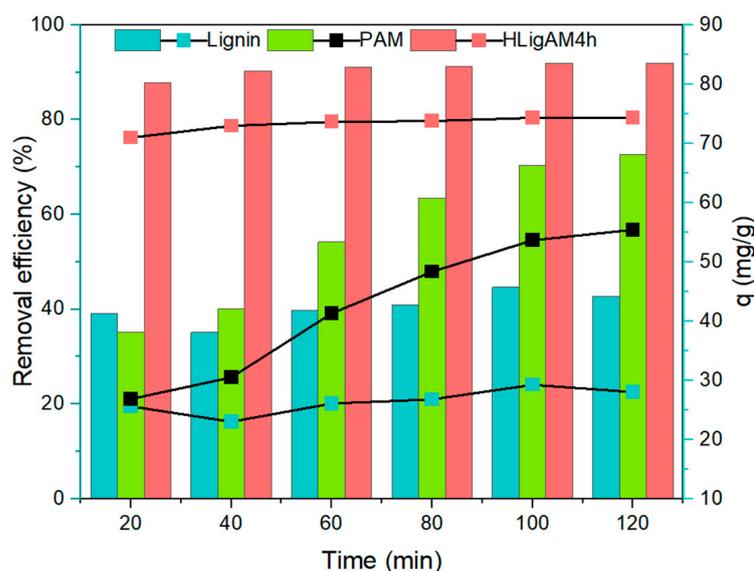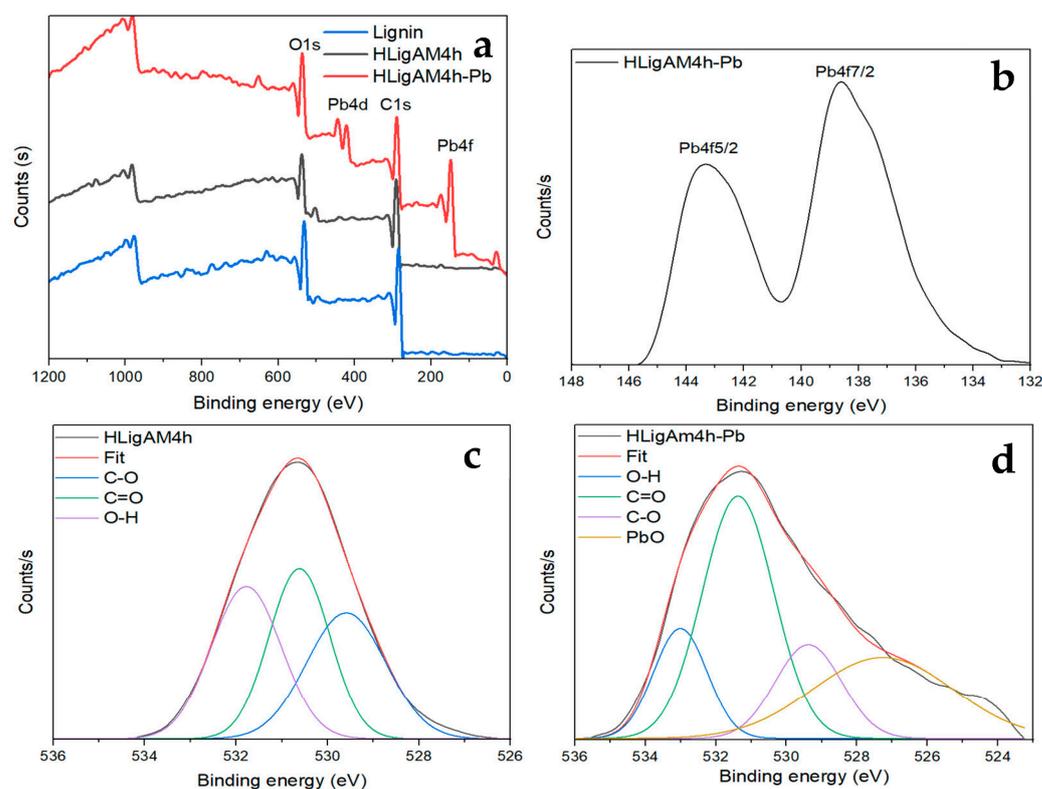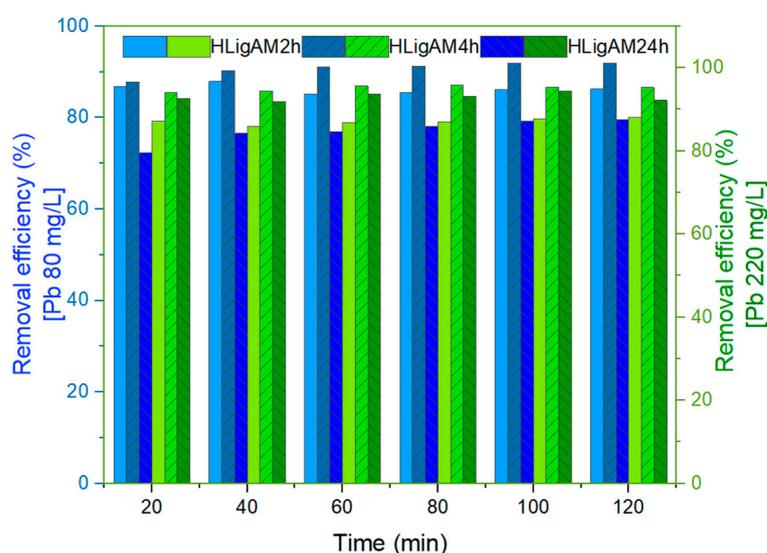**Figure 9.** Comparison of removal efficiencies and adsorption capacities for lignin, PAM, and HLigAM4h.

Figure 10. (**a**) XPS spectra before and after adsorption of Pb^{2+}, (**b**) Pb4f XPS spectrum, (**c**,**d**) O1s spectra before and after adsorption of Pb^{2+}, respectively.

3.3.2. Effect of Lignin Modification Time

Pb^{2+} removal experiments from water using lignin-modified copolymers obtained at 2, 4, and 24 h, with initial Pb^{2+} concentrations of 80 and 220 mg L^{-1}, are shown in Figure 11. Removal efficiencies higher than 85% are obtained after 20 min for materials HLigAM2h and HLigAM4h. Maximum removal efficiencies are reached at about 60 min. These efficiencies are 85, 91 and 77% for HLigAM2h, HLigAM4h, and HLigAM24h at 80 mg L^{-1}, respectively; and 87, 96, and 94% for HLigAM2h, HligAM4h, and HligAM24h at 220 mg L^{-1}, respectively. Removal efficiencies and adsorption capacities are improved

by increasing the initial concentration of Pb^{2+}. These improvements may be explained by better interaction and increased mass transfer between Pb ions and the surface of the materials [26,27]. The three lignin-modified copolymers have high removal efficiencies; however, the best performance is obtained with HLigAM4h. The maximum adsorption capacity for HLigAM4h was obtained using an initial concentration of 220 mg L^{-1}, which corresponds to 209.82 mg g^{-1}. This adsorption capacity is higher than the capacities reported for bioadsorbents synthesized by different polymerization techniques, such as the case of lignin microspheres prepared by inverse suspension copolymerization with polyethylenimine, where an adsorption capacity of 33.9 mg g^{-1} was reported [29]. In the case of graft copolymerization of cellulose acetate with acrylic acid and acrylamide, the adsorption capacity was 66.67 mg g^{-1} [55]. Finally, in the case of poly(acrylic acid) grafted onto an acid-pretreated alkali lignin-hydrogel prepared by crosslinking free radical copolymerization, the adsorption capacity was 1.076 mmol g^{-1} [19].

Figure 11. Comparison of removal efficiencies of the synthesized copolymers.

3.3.3. Effect of Heating Source

It has been reported that the use of microwave irradiation as a heating source in polymerization studies decreases considerably the time required to complete the polymerization [40]. That is why we also conducted lignin modification using microwave irradiation as heating source. Figure 12 shows a comparison of Pb^{2+} adsorption efficiencies using modified materials obtained with thermal (H-LigAM4h) and microwave promoted heating (HLigAM-MW5). Removals efficiencies of 81% and 86% were archived at 20 and 60 min when the initial concentration of Pb^{2+} was 80 mg L^{-1}, using HLigAM-MW5. Similar results were obtained with HLigAM4h. In the case of Pb^{2+} = [220 mg L^{-1}], efficiencies of 72 and 80% were obtained at 20 and 60 min, respectively. It is observed that in the case of modified lignin copolymers obtained by using microwave irradiation their adsorption capacity decreases as the initial concentration of Pb^{2+} increases. In contrast, the opposite effect is observed in modified copolymers synthesized by thermal heating, where the reaction time is longer. This dissimilar behavior may be caused by a lower grating degree or by smaller grafted branches.
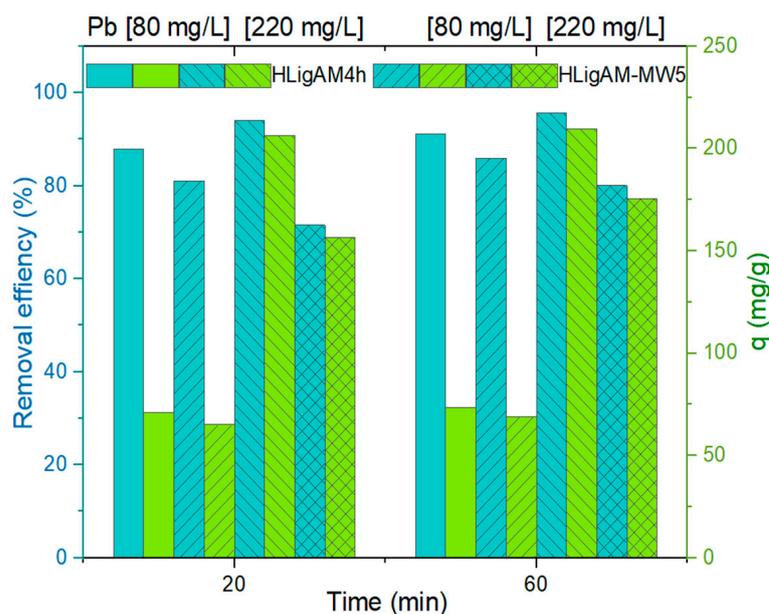
Figure 12. Comparison of removal efficiencies and adsorption capacities of HLigAM4h and HLigMW5.

4. Conclusions

Modified lignin copolymers obtained by grafting of crosslinked PAM onto Kraft lignin using conventional and microwave heating were successfully synthesized. The obtained materials were evaluated as adsorbent materials for the removal of Pb^{2+} from a solution of lead in water. Copolymerization time does not seem to be a determining factor in the adsorption of Pb^{2+} since high removal efficiencies were observed at the lowest evaluated time of 2 h. A removal efficiency of 94% at 20 min of the adsorption experiment was obtained when using HLigAM4h at an initial Pb^{2+} concentration of 220 mg L^{-1}. A maximum removal efficiency of 96% and a maximum adsorption capacity of 209.82 mg g^{-1} were obtained. The separation of copolymers after the adsorption experiment was simple due to the fact that the material did not dissolve and almost all the material sedimented when the agitation was turned off, which is a plus in the potential use of these materials for lead removal purposes. The modified lignin copolymer synthesized by microwave heating showed good Pb^{2+} removal performance, with a removal efficiency of 86%.

References

1. Sternberg, J.; Sequerth, O.; Pilla, S. Green chemistry design in polymers derived from lignin: Review and perspective. *Prog. Polym. Sci.* **2021**, *113*, 101344. [CrossRef]
2. Araújo, D.M.F.; Filho, I.J.D.C.; Santos, T.; Pereira, D.T.M.; Marques, D.S.C.; Lima, A.d.C.A.d.; de Aquino, T.M.; Rocha, G.J.D.M.; de Lima, M.D.C.A.; Nogueira, F. Biological activities and physicochemical characterization of alkaline lignins obtained from branches and leaves of Buchenavia viridiflora with potential pharmaceutical and biomedical applications. *Int. J. Biol. Macromol.* **2022**, *219*, 224–245. [CrossRef]
3. Morales-Huerta, J.C.; Hernández-Meléndez, O.; Garcés-Sandoval, F.I.; Montiel, C.; Hernández-Luna, M.G.; Manero, O.; Bárzana, E.; Vivaldo-Lima, E. Modeling of Pretreatment and Combined Alkaline and Enzymatic Hydrolyses of Blue Agave Bagasse in Corotating Twin-Screw Extruders. *Macromol. React. Eng.* **2022**, *16*, 2100059. [CrossRef]
4. An, L.; Si, C.; Bae, J.H.; Jeong, H.; Kim, Y.S. One-step silanization and amination of lignin and its adsorption of Congo red and Cu(II) ions in aqueous solution. *Int. J. Biol. Macromol.* **2020**, *159*, 222–230. [CrossRef] [PubMed]
5. Bao, X.; Fan, X.; Yu, Y.; Wang, Q.; Wang, P.; Yuan, J. Graft modification of lignin-based cellulose via enzyme-initiated reversible addition-fragmentation chain transfer (RAFT) polymerization and free-radical coupling. *Int. J. Biol. Macromol.* **2019**, *144*, 267–278. [CrossRef]
6. Ganewatta, M.S.; Lokupitiya, H.N.; Tang, C. Lignin Biopolymers in the Age of Controlled Polymerization. *Polymers* **2019**, *11*, 1176. [CrossRef]
7. Ge, Y.; Li, Z. Application of Lignin and Its Derivatives in Adsorption of Heavy Metal Ions in Water: A Review. *ACS Sustain Chem. Eng.* **2018**, *6*, 7181–7192. [CrossRef]
8. Kong, F.; Wang, S.; Price, J.T.; Konduri, M.K.; Fatehi, P. Water soluble kraft lignin–acrylic acid copolymer: Synthesis and characterization. *Green Chem.* **2015**, *17*, 4355–4366. [CrossRef]
9. Xu, Q.; Bai, Y.; Zhao, X.; Ren, M.; Wang, S.; Kong, F. Synthesis and characterization of an amphiphilic lignin-based cationic surfactant. *Ind. Crops Prod.* **2021**, *164*, 113376. [CrossRef]
10. Li, J.; Li, H.; Yuan, Z.; Fang, J.; Chang, L.; Zhang, H.; Li, C. Role of sulfonation in lignin-based material for adsorption removal of cationic dyes. *Int. J. Biol. Macromol.* **2019**, *135*, 1171–1181. [CrossRef]
11. Li, Y.; Wang, F.; Miao, Y.; Mai, Y.; Li, H.; Chen, X.; Chen, J. A lignin-biochar with high oxygen-containing groups for adsorbing lead ion prepared by simultaneous oxidization and carbonization. *Bioresour. Technol.* **2020**, *307*, 123165. [CrossRef]
12. Luo, S.; Cao, J.; McDonald, A.G. Esterification of industrial lignin and its effect on the resulting poly(3-hydroxybutyrate-co-3-hydroxyvalerate) or polypropylene blends. *Ind. Crops Prod.* **2017**, *97*, 281–291. [CrossRef]
13. Zhou, H.; Shi, X.; Wu, W.; An, X.; Tian, Y.; Qiao, Y. Facile preparation of lignosulfonate/N-methylaniline composite and its application in efficient removal of Cr(VI) from aqueous solutions. *Int. J. Biol. Macromol.* **2020**, *154*, 1194–1204. [CrossRef] [PubMed]
14. Liu, X.; Xu, Y.; Yu, J.; Li, S.; Wang, J.; Wang, C.; Chu, F. Integration of lignin and acrylic monomers towards grafted copolymers by free radical polymerization. *Int. J. Biol. Macromol.* **2014**, *67*, 483–489. [CrossRef] [PubMed]
15. Vega-hernández, M.Á.; Cano-díaz, G.S.; Vivaldo-lima, E.; Rosas-aburto, A.; Hernández-luna, M.G.; Martinez, A.; Palacios-alquisira, J.; Mohammadi, Y.; Penlidis, A. A Review on the Synthesis, Characterization and Modeling of Polymer Grafting. *Processes* **2021**, *9*, 375. [CrossRef]
16. Pourmahdi, M.; Abdollahi, M.; Nasiri, A. Effect of lignin source and initiation conditions on graft copolymerization of lignin with acrylamide and performance of graft copolymer as additive in water-based drilling fluid. *J. Pet. Sci. Eng.* **2023**, *220*, 111253. [CrossRef]
17. Aldajani, M.; Alipoormazandarani, N.; Kong, F.; Fatehi, P. Acid hydrolysis of kraft lignin-acrylamide polymer to improve its flocculation affinity. *Sep. Purif. Technol.* **2020**, *258*, 117964. [CrossRef]
18. Wu, W.; Qi, J.; Fang, J.; Lyu, G.; Yuan, Z.; Wang, Y.; Li, H. One-pot preparation of lignin-based cationic flocculant and its application in dye wastewater. *Colloids Surf. A Physicochem. Eng. Asp.* **2022**, *654*, 130082. [CrossRef]
19. Liu, M.; Liu, Y.; Shen, J.; Zhang, S.; Liu, X.; Chen, X.; Ma, Y.; Ren, S.; Fang, G.; Li, S.; et al. Simultaneous removal of Pb^{2+}, Cu^{2+} and Cd^{2+} ions from wastewater using hierarchical porous polyacrylic acid grafted with lignin. *J. Hazard. Mater.* **2020**, *392*, 122208. [CrossRef]
20. Lee, K.E.; Morad, N.; Teng, T.T.; Poh, B.T. Development, Characterization and the Application of Hybrid Ma-terials in Coagulation/Flocculation of Wastewater: A Review. *Chem. Eng. J.* **2012**, *203*, 370–386. [CrossRef]
21. Guo, K.; Gao, B.; Yue, Q.; Xu, X.; Li, R.; Shen, X. Characterization and performance of a novel lignin-based flocculant for the treatment of dye wastewater. *Int. Biodeterior. Biodegrad.* **2018**, *133*, 99–107. [CrossRef]

22. Feng, X.; Wan, J.; Deng, J.; Qin, W.; Zhao, N.; Luo, X.; He, M.; Chen, X. Preparation of acrylamide and carboxymethyl cellulose graft copolymers and the effect of molecular weight on the flocculation properties in simulated dyeing wastewater under different pH conditions. *Int. J. Biol. Macromol.* **2019**, *155*, 1142–1156. [CrossRef]

23. Zhu, H.; Zhang, Y.; Yang, X.; Shao, L.; Zhang, X.; Yao, J. Polyacrylamide grafted cellulose as an eco-friendly flocculant: Key factors optimization of flocculation to surfactant effluent. *Carbohydr. Polym.* **2016**, *135*, 145–152. [CrossRef] [PubMed]

24. Chen, W.; Zhang, F.; Tang, Q.; Du, B.; Ma, D.; Zhao, Z.; Fan, L.; Luo, H.; Zhao, Z.; Huang, X.; et al. Evaluating the performance of bridging-assembly chelating flocculant for heavy metals removal: Role of branched architectures. *Chemosphere* **2021**, *289*, 133260. [CrossRef] [PubMed]

25. Gupta, A.; Sharma, V.; Sharma, K.; Kumar, V.; Choudhary, S.; Mankotia, P.; Kumar, B.; Mishra, H.; Moulick, A.; Ekielski, A.; et al. A Review of Adsorbents for Heavy Metal Decontamination: Growing Approach to Wastewater Treatment. *Materials* **2021**, *14*, 4702. [CrossRef] [PubMed]

26. Wang, B.; Wen, J.-L.; Sun, S.-L.; Wang, H.-M.; Wang, S.-F.; Liu, Q.-Y.; Charlton, A.; Sun, R.-C. Chemosynthesis and structural characterization of a novel lignin-based bio-sorbent and its strong adsorption for Pb (II). *Ind. Crops Prod.* **2017**, *108*, 72–80. [CrossRef]

27. Shi, X.; Qiao, Y.; An, X.; Tian, Y.; Zhou, H. High-capacity adsorption of Cr(VI) by lignin-based composite: Characterization, performance and mechanism. *Int. J. Biol. Macromol.* **2020**, *159*, 839–849. [CrossRef]

28. Popovic, A.L.; Rusmirovic, J.D.; Velickovic, Z.; Radovanovic, Z.; Ristic, M.; Pavlovic, V.P.; Marinkovic, A.D. Novel amino-functionalized lignin microspheres: High performance biosorbent with enhanced capacity for heavy metal ion removal. *Int. J. Biol. Macromol.* **2020**, *156*, 1160–1173. [CrossRef]

29. Ge, Y.; Qin, L.; Li, Z. Lignin microspheres: An effective and recyclable natural polymer-based adsorbent for lead ion removal. *Mater. Des.* **2016**, *95*, 141–147. [CrossRef]

30. Jiao, G.-J.; Ma, J.; Li, Y.; Jin, D.; Zhou, J.; Sun, R. Removed heavy metal ions from wastewater reuse for chemiluminescence: Successive application of lignin-based composite hydrogels. *J. Hazard. Mater.* **2021**, *421*, 126722. [CrossRef]

31. Zhang, F.; Wang, B.; Jie, P.; Zhu, J.; Cheng, F. Preparation of chitosan/lignosulfonate for effectively removing Pb(II) in water. *Polymer* **2021**, *228*, 123878. [CrossRef]

32. Fang, R.; Cheng, X.-S.; Fu, J.; Zheng, Z.-B. Research on the Graft Copolymerization of EH-lignin with acrylamide. *Nat. Sci.* **2009**, *01*, 17–22. [CrossRef]

33. Wang, S.; Sun, Y.; Kong, F.; Yang, G.; Fatehi, P. Preparation and Characterization of Lignin-Acrylamide Copolymer as a Paper Strength Additive. *Bioresources* **2015**, *11*, 1765–1783. [CrossRef]

34. Li, Z.; Kong, Y.; Ge, Y. Synthesis of porous lignin xanthate resin for Pb^{2+} removal from aqueous solution. *Chem. Eng. J.* **2015**, *270*, 229–234. [CrossRef]

35. Li, Y.; Zhao, R.; Pang, Y.; Qiu, X.; Yang, D. Microwave-assisted synthesis of high carboxyl content of lignin for enhancing adsorption of lead. *Colloids Surfaces A Physicochem. Eng. Asp.* **2018**, *553*, 187–194. [CrossRef]

36. Du, B.; Chai, L.; Zheng, Q.; Liu, Y.; Wang, X.; Chen, X.; Zhai, S.; Zhou, J.; Sun, R.-C. Designed synthesis of multifunctional lignin-based adsorbent for efficient heavy metal ions removal and electromagnetic wave absorption. *Int. J. Biol. Macromol.* **2023**, *234*, 123668. [CrossRef]

37. Dlamini, D.S.; Mishra, A.K.; Mamba, B.B. Kinetic and equilibrium studies of the removal of Pb^{2+} from aqueous solutions using Na_2SO_4-EVA/Cloisite® 20A composite. *Mater. Chem. Phys.* **2012**, *133*, 369–375. [CrossRef]

38. Sun, Y.; Ma, Z.; Xu, X.; Liu, X.; Liu, L.; Huang, G.; Liu, L.; Wang, H.; Song, P. Grafting Lignin with Bioderived Polyacrylates for Low-Cost, Ductile, and Fully Biobased Poly(lactic acid) Composites. *ACS Sustain. Chem. Eng.* **2020**, *8*, 2267–2276. [CrossRef]

39. Sinnwell, S.; Ritter, H. Microwave assisted hydroxyalkylamidation of poly(ethylene-co-acrylic acid) and formation of grafted poly(ε-caprolactone) side chains. *J. Polym. Sci. A Polym. Chem.* **2007**, *45*, 3659–3667. [CrossRef]

40. Sincari, V.; Petrova, S.L.; Konefał, R.; Hruby, M.; Jäger, E. Microwave-assisted RAFT polymerization of N-(2-hydroxypropyl) methacrylamide and its relevant copolymers. *React. Funct. Polym.* **2021**, *162*, 104875. [CrossRef]

41. Zhang, X.; Li, Y.; Hou, Y. Preparation of magnetic polyethylenimine lignin and its adsorption of Pb(II). *Int. J. Biol. Macromol.* **2019**, *141*, 1102–1110. [CrossRef] [PubMed]

42. Wang, H.; Song, J.; Yan, M.; Li, J.; Yang, J.; Huang, M.; Zhang, R. Waste lignin-based cationic flocculants treating dyeing wastewater: Fabrication, performance, and mechanism. *Sci. Total Environ.* **2023**, *874*, 162383. [CrossRef] [PubMed]

43. Cui, G.; Wang, X.; Xun, J.; Lou, T. Microwave assisted synthesis and characterization of a ternary flocculant from chitosan, acrylamide and lignin. *Int. Biodeterior. Biodegrad.* **2017**, *123*, 269–275. [CrossRef]

44. Wang, X.; Zhang, Y.; Hao, C.; Dai, X.; Zhou, Z.; Si, N. Ultrasonic-assisted synthesis of aminated lignin by a Mannich reaction and its decolorizing properties for anionic azo-dyes. *RSC Adv.* **2014**, *4*, 28156–28164. [CrossRef]

45. Liu, X.; Gao, C.; Fu, C.; Xi, Y.; Fatehi, P.; Zhao, J.R.; Wang, S.; Gibril, M.E.; Kong, F. Preparation and Performance of Lignin-Based Multifunctional Superhydrophobic Coating. *Molecules* **2022**, *27*, 1440. [CrossRef] [PubMed]

46. Wang, B.; Hong, S.; Sun, Q.; Cao, X.; Yu, S.; Sun, Z.; Yuan, T.-Q. Performance regulation of lignin-based flocculant at the practical molecular level by fractionation. *Sep. Purif. Technol.* **2022**, *299*, 121670. [CrossRef]

47. Vilén, E.M.; Sandström, C. NMR Study on the Interaction of Trehalose with Lactose and Its Effect on the Hydrogen Bond Interaction in Lactose. *Molecules* **2013**, *18*, 9735–9754. [CrossRef] [PubMed]

48. Gan, L.H.; Zhou, M.S.; Qiu, X.Q. Preparation of Water-Soluble Carboxymethylated Lignin from Wheat Straw Alkali Lignin. *Adv. Mater. Res.* **2012**, *550–553*, 1293–1298. [CrossRef]
49. Konduri, M.K.; Kong, F.; Fatehi, P. Production of carboxymethylated lignin and its application as a dispersant. *Eur. Polym. J.* **2015**, *70*, 371–383. [CrossRef]
50. Liang, J.; Li, X.; Yu, Z.; Zeng, G.; Luo, Y.; Jiang, L.; Yang, Z.; Qian, Y.; Wu, H. Amorphous MnO_2 Modified Biochar Derived from Aerobically Composted Swine Manure for Adsorption of Pb(II) and Cd(II). *ACS Sustain. Chem. Eng.* **2017**, *5*, 5049–5058. [CrossRef]
51. Zhang, Y.; Ni, S.; Wang, X.; Zhang, W.; Lagerquist, L.; Qin, M.; Willför, S.; Xu, C.; Fatehi, P. Ultrafast adsorption of heavy metal ions onto functionalized lignin-based hybrid magnetic nanoparticles. *Chem. Eng. J.* **2019**, *372*, 82–91. [CrossRef]
52. Jiang, S.; Yan, L.; Wang, R.; Li, G.; Rao, P.; Ju, M.; Jian, L.; Guo, X.; Che, L. Recyclable nitrogen-doped biochar via low-temperature pyrolysis for enhanced lead(II) removal. *Chemosphere* **2022**, *286*, 131666. [CrossRef] [PubMed]
53. Liu, C.; Li, Y.; Hou, Y. Preparation of a Novel Lignin Nanosphere Adsorbent for Enhancing Adsorption of Lead. *Molecules* **2019**, *24*, 2704. [CrossRef] [PubMed]
54. Fan, Y.; Wang, H.; Deng, L.; Wang, Y.; Kang, D.; Li, C.; Chen, H. Enhanced adsorption of Pb(II) by nitrogen and phosphorus co-doped biochar derived from Camellia oleifera shells. *Environ. Res.* **2020**, *191*, 110030. [CrossRef]
55. Abdelwahab, N.A.; Ammar, N.S.; Ibrahim, H.S. Graft copolymerization of cellulose acetate for removal and recovery of lead ions from wastewater. *Int. J. Biol. Macromol.* **2015**, *79*, 913–922. [CrossRef]